

## ARTICLE OPEN

Anisotropy of magnetic interactions and symmetry of the order parameter in unconventional superconductor  $\text{Sr}_2\text{RuO}_4$ Bongjae Kim<sup>1</sup>, Sergii Khmelevskiy<sup>1,2</sup>, Igor I. Mazin<sup>3</sup>, Daniel F. Agterberg<sup>4</sup> and Cesare Franchini<sup>1</sup>

$\text{Sr}_2\text{RuO}_4$  is the best candidate for spin-triplet superconductivity, an unusual and elusive superconducting state of fundamental importance. In the last three decades,  $\text{Sr}_2\text{RuO}_4$  has been very carefully studied and despite its apparent simplicity when compared with strongly correlated high- $T_c$  cuprates, for which the pairing symmetry is understood, there is no scenario that can explain all the major experimental observations, a conundrum that has generated tremendous interest. Here, we present a density-functional-based analysis of magnetic interactions in  $\text{Sr}_2\text{RuO}_4$  and discuss the role of magnetic anisotropy in its unconventional superconductivity. Our goal is twofold. First, we access the possibility of the superconducting order parameter rotation in an external magnetic field of 200 Oe, and conclude that the spin-orbit interaction in this material is several orders of magnitude too strong to be consistent with this hypothesis. Thus, the observed invariance of the Knight shift across  $T_c$  has no plausible explanation, and casts doubt on using the Knight shift as an ultimate litmus paper for the pairing symmetry. Second, we propose a quantitative double-exchange-like model for combining itinerant fermions with an anisotropic Heisenberg magnetic Hamiltonian. This model is complementary to the Hubbard-model-based calculations published so far, and forms an alternative framework for exploring superconducting symmetry in  $\text{Sr}_2\text{RuO}_4$ . As an example, we use this model to analyze the degeneracy between various  $p$ -triplet states in the simplest mean-field approximation, and show that it splits into a single and two doublets with the ground state defined by the competition between the “Ising” and “compass” anisotropic terms.

npj Quantum Materials (2017)2:37; doi:10.1038/s41535-017-0041-8

## INTRODUCTION

Superconductivity in  $\text{Sr}_2\text{RuO}_4$ , even though it occurs at a rather low temperature, has been attracting attention comparable to that attached to high-temperature superconductors.<sup>1</sup> For many years the dominant opinion was that it represents a unique example of a chiral triplet pairing state.<sup>2–5</sup> Interestingly, the original premise that led to this hypothesis was the presumed proximity of  $\text{Sr}_2\text{RuO}_4$  to ferromagnetism, and thus it was touted as a three-dimensional analogue of  $^3\text{He}$ .<sup>6, 7</sup> It was soon discovered, first theoretically,<sup>8</sup> and then experimentally,<sup>9</sup> that the leading instability occurs in an antiferromagnetic, not ferromagnetic channel, and thus a spin-fluctuation exchange (FLEX) in the Berk-Schrieffer spirit would normally lead to a  $d$ -wave, not  $p$ -wave superconductivity.

The issue seems to have been decided conclusively when the Knight shift on Ru was shown to be temperature-independent across  $T_c$ ,<sup>2</sup> and later also on O,<sup>3</sup> and the neutron-measured spin-susceptibility was found to be roughly constant across the transition as well.<sup>4</sup> The chiral  $p$ -wave state with an order parameter  $\mathbf{d} = \text{const}(x + iy)\hat{\mathbf{z}}$ , where the Cooper pair spins can freely rotate in-plane, is the only state that could have this property. Moreover, since in this state spins are confined in the  $xy$  plane, the Knight shift in a magnetic field parallel to  $\hat{\mathbf{z}}$  is supposed to drop below  $T_c$  in pretty much the same manner as in singlet superconductors. Nonetheless, when eventually this experiment was performed,<sup>10</sup> it appeared that  $K_z$  is also independent of temperature. The authors of ref. 10 attempted to reconcile the

accepted pairing symmetry with their experiment, by assuming that the experimental magnetic field of 200 Oe is affecting drastically the pairing state and converting it to  $\mathbf{d} = f(x, y)\hat{\mathbf{y}}$  (or the corresponding  $x \leftrightarrow y$  partner state). One goal of our paper is to estimate whether this hypothesis is tenable with realistic material parameters.

It is worth noting that the invariance of the in-plane susceptibility is the only experiment consistent *exclusively* with a chiral  $p$ -state (CpS). Some probes indicate chirality ( $\mu\text{SR}$  detects spontaneous currents below  $T_c$ <sup>5</sup>), while others indicate breaking of time-reversal symmetry,<sup>11</sup> but the triplet parity is not, in principle, necessary to explain these experiments. For instance, the singlet chiral state  $\Delta = \text{const}(xz + iyz)$ , or even  $\Delta = \text{const}(x^2 + y^2 + iaxy)$ , which is not chiral (although this second state would require two-phase transitions with decreasing temperature, which has never been detected), but breaks the time reversal symmetry, are other admissible candidates. Josephson junction experiments<sup>12</sup> suggested that the order parameter changes sign under the  $(x, y) \leftrightarrow (-x, -y)$  transformation, which is consistent with a CpS, but also with other order parameters.<sup>13</sup>

Spin-orbit (SO) coupling plays an important role not only in selecting between different triplet states (chiral vs. planar), but also in the structure of the chiral state itself. For instance, in  $\text{Cu}_x\text{Bi}_2\text{Se}_3$ , instead of the expected chiral state, a nematic spin-triplet state was observed.<sup>14, 15</sup> Indeed, in  $\text{Cu}_x\text{Bi}_2\text{Se}_3$  the large SO coupling necessarily implies that a  $\mathbf{d} = \text{const}(x + iy)\hat{\mathbf{z}}$  induces also an in-plane  $\mathbf{d}$ -vector component  $\text{const}(\hat{\mathbf{x}} + i\hat{\mathbf{y}})\hat{\mathbf{z}}$ .<sup>16</sup> This in-plane

<sup>1</sup>Faculty of Physics and Center for Computational Materials Science, University of Vienna, Vienna A-1090, Austria; <sup>2</sup>Center for Computational Materials Science, Institute for Applied Physics, Vienna University of Technology, Wiedner Hauptstrasse 8 - 10, Vienna 1040, Austria; <sup>3</sup>Code 6393, Naval Research Laboratory, Washington, DC 20375, USA and

<sup>4</sup>Department of Physics, University of Wisconsin, Milwaukee, WI 53201, USA

Correspondence: Cesare Franchini (cesare.franchini@univie.ac.at)

Bongjae Kim and Sergii Khmelevskiy contributed equally to this work.

Received: 6 February 2017 Revised: 1 June 2017 Accepted: 12 June 2017

Published online: 04 July 2017

component leads to a non-unitary pairing state, which is not energetically favored in weak coupling,<sup>17</sup> and, instead, the lower-symmetry nematic state with  $\mathbf{d} = c_1x\hat{\mathbf{z}} + c_2z\hat{\mathbf{x}}$  is realized. In principle, similar physics must occur in  $\text{Sr}_2\text{RuO}_4$ , but there the corresponding induced in-plane  $\mathbf{d}$ -vector component should be much smaller, thus allowing for a chiral  $p$ -wave state to exist. However, this is a quantitative, not qualitative difference, and needs a better understanding of the role of SO coupling.

Finally, recent years have brought about an array of experiments that are actually *inconsistent* with the CpS. One prediction of a CpS is the existence of edge states at boundaries and at domain walls.<sup>18–20</sup> However, no evidence for these edge states has been found.<sup>19, 21</sup> There are a variety of predictions about the response of CpS to in-plane magnetic fields that have not been observed experimentally. In particular, it is known that a finite in-plane magnetic field should lead to two superconducting transitions as temperature is reduced<sup>22, 23</sup> and that the slope of the upper critical field with temperature at  $T_c$  should depend on the in-plane field direction (this is only true for pairing states that can break time-reversal symmetry).<sup>23, 24</sup> In addition, several different probes indicate behavior resembling substantial Pauli paramagnetic effects (see ref. 25 for discussion and original references). The latest cloud on the CpS sky appeared because of the uniaxial strain experiments. For the CpS (or, in fact, any other two-component state) the critical temperature,  $T_c$ , under an orthorhombic stress must change linearly with the strain (the  $x\hat{\mathbf{z}}$  and  $y\hat{\mathbf{z}}$  state will not degenerate any more, and the splitting is linear in strain). In the experiment<sup>26</sup>  $T_c$  varies at least quadratically (more likely, quartically), whereas the linear term is absent within the experimental accuracy, and only one, very well-expressed specific heat jump,  $\Delta C$ , has been observed, with no trace of a second transition even while the critical temperature changes a lot (Note: Li, Gibbs, Mackenzie, Hicks, and Nicklas (2017). Heat capacity measurements of  $\text{Sr}_2\text{RuO}_4$  under uniaxial stress. Unpublished (reported at the APS March Meeting, New Orleans)). Moreover, it was established that both  $T_c$  and the  $\Delta C$  variations trace the changes in the density of states, and peak when the Fermi level passes the van Hove singularities at the  $X$  or  $Y$  points. This observation is particularly important, because, by symmetry, the superconducting gap in a triplet channel in a tetragonal superconductor is identically zero at  $X$  and  $Y$  (it need not be zero at a finite  $k_z$ , but in a highly 2D material like  $\text{Sr}_2\text{RuO}_4$  it will be still very small by virtue of continuity). Correspondingly, one expects these van Hove singularities to have little effect on superconductivity. A slightly more subtle, but even more convincing argument against triplet pairing in ref. 26 is related to the reduced critical field anisotropy. Finally, a recent detailed study of thermal conductivity has concluded that a  $d$ -wave state is by far better consistent with the thermal transport than the CpS.<sup>27</sup>

In fact, only one fact unambiguously points toward the CpS: the invariance of the spin susceptibility in the in-plane magnetic field—but, as discussed above, the analogous experiment for the out-of-plane field *also* shows such an invariance. Thus, our acceptance of the nuclear magnetic resonance data as an ultimate proof of the CpS hinges upon the possibility of a magnetic field  $B \approx 200$  Oe (0.02 T, or 13 mK in temperature units) to overcome the energy difference between the helical ( $\mathbf{d} \perp \hat{\mathbf{z}}$ ) and chiral ( $\mathbf{d} \parallel \hat{\mathbf{z}}$ ) states. One can show (the derivation is presented below) that this implies that the two states, whose energy difference comes from the SO interaction, are nearly degenerate with the accuracy  $\delta \approx 10^{-7}$  K  $\approx 10^{-10}$   $\lambda$ , where  $\lambda \approx 100$  meV is the SO constant. Moreover, it is often claimed that the solution of other paradoxes outlined above may be obtained (although nobody has convincingly succeeded in that) in a formalism where the relativistic effects would be fully accounted for, since the separation between singlet and triplet channels is only possible in terms of the full angular momentum, rather than just electron spins.

## RESULTS AND DISCUSSION

In order to illustrate how SO coupling affects the core assumption of the field-induced  $\mathbf{d}$ -vector rotation, let us show a simple back-of-the-envelope calculation: suppose that the one-electron Hamiltonian has a relativistic term of the order of  $\kappa M_z^2$ . The physical meaning of this term is that in the *normal* state when  $n$  electron spins are confined in the  $xy$  plane (as opposed to be parallel to  $z$ ), this affects the exchange part of the effective crystal potential, and, correspondingly, one-electron energies. The change is proportional to  $n$ , and so is the number of affected one-electron states, leading to an energy loss of the order of  $\kappa n^2$ , where  $\kappa$  is the magnetic anisotropy scale that is determined by the SO coupling. One way in which this energy contribution manifests itself is the conventional magnetic anisotropy in a spin-ordered state in which case  $n \approx M/\mu_B$ . However, the same “feedback” effect must be present in a triplet superconducting state. The number of electrons bound in Cooper pairs and thus forced to be either parallel or perpendicular to  $z$  can be estimated as  $n \sim \Delta N$ , where  $\Delta$  is some average superconducting gap, and  $N$  is the density of states, which has been experimentally measured to be about 8 states/spin/Ru/eV.<sup>1</sup> Assuming  $\Delta \sim 7.5$  K, we estimate  $n \sim 0.005$  e/Ru. If the magnetic anisotropy scale  $\kappa$  is of the order of 10 K (we will show later that this is the case), then the total energy loss incurred by rotating the spins of the Cooper pairs is  $\Delta E_{sc} \approx 2 \times 10^{-4}$  K (this is smaller than various model estimates of the change in  $T_c$ , as reviewed in ref. 28; we use the above estimate because we wanted to have a conservative *lower* bound on  $\Delta E_{sc}$  and a *model-independent* estimate of the energy, and not simply a critical temperature difference, since the latter may, in principle, dramatically differ from the former). This seems like a small number, but we shall compare it with the energy gained by allowing screening of an external field of 200 Oe by Cooper pairs, which is  $\Delta E_{mag} \approx \mu_B^2 B^2 N \approx 10^{-7}$  K. This is *four orders of magnitude* smaller than the estimated loss of superconducting energy. In other words, to allow for the presumed  $d$ -vector rotation, various relativistic effects must fortuitously cancel each other with a  $10^{-3}$  accuracy. Note that in ref. 28, instead,  $\Delta T_c$  was compared with the Zeeman splitting,  $\mu_B B$ , but this comparison is hardly relevant at all for the problem at hand; the correct way is to compare the energy gain with the energy loss.

This simple estimate emphasizes the importance of getting a handle of the type and scale of relativistic effects in  $\text{Sr}_2\text{RuO}_4$ . So far all efforts in this direction have been performed either within simplified models or by educated guesses from the experiment.<sup>29–33</sup> The goal of this paper is to address the issue from a first-principle perspective. It is known that this approach correctly describes (only slightly underestimating) the SO interactions<sup>34</sup> (our SO splitting is exactly the same as calculated in that reference, 90 meV), and, by comparing the Fourier transform of the calculated exchange interaction with the experimentally measured  $\mathbf{q}$ -dependent spin susceptibility, we observe that the latter is also well reproduced. The only serious problem with this approach is that it overestimates the tendency to magnetic ordering for a given set of magnetic interactions because of the mean field nature of the density functional theory (DFT). Thus, we start with a realistic paramagnetic state of  $\text{Sr}_2\text{RuO}_4$ , using the alloy analogy model in the first-principles DFT framework and calculate the isotropic exchange interactions (see “Methods”). The Fourier transform of these interactions gives us the shape of the full spin susceptibility in the momentum space; as expected, this is peaked at the nesting vector  $\mathbf{q}_3 = (1, 1, 0) \frac{2\pi}{3a}$ , in agreement with the experiment. Next, we calculate the mean-field energy of several ordered magnetic states, all characterized by the same wave vector  $\mathbf{q} = \mathbf{q}_3$ , and degenerate without SO interaction. This shall allow us to calculate nearest neighbor (NN) relativistic Ising terms (see below). Finally, we calculate magnetic anisotropy for the  $\mathbf{q} = (1, 0, 0) \frac{\pi}{a}$  states, which breaks the tetragonal symmetry, and from

there we extract the NN compass exchange (see “Methods”). The energy scale of magnetic anisotropy appears rather large, which not only renders the hypothesis of a  $\mathbf{d}$ -vector rotation unlikely, but also supports the idea that anisotropic interactions must be properly accounted for before drawing conclusions from the experiment. The set of interactions that we derived should serve as a launching pad and testbed for model calculation of the superconducting properties. We maintain that a model where all interelectron interactions are absorbed into spin–spin interactions (with Hund’s coupling between the spins and non-interacting electrons) is complementary to the widely used Hubbard-model and at least as realistic.

Experimentally,  $\text{Sr}_2\text{RuO}_4$  shows no sign of magnetic ordering down to the low temperatures. However, neutron diffraction studies have revealed<sup>35–37</sup> spin-fluctuations in the paramagnetic state with a characteristic nearly commensurate wave vector  $\mathbf{q} = (0.3, 0.3, 0) \frac{2\pi}{a}$ , close to  $\mathbf{q}_3 = (1, 1, 0) \frac{2\pi}{3a}$ , which persist even at the room temperature.<sup>38</sup> The DFT, being a static mean field theory (by some criteria, the best such theory possible), overestimates the tendency to magnetism. In its generalized gradient approximation flavor DFT stabilizes even ferromagnetic order, albeit with small moments.<sup>39</sup> Unsurprisingly, spin-density waves (SDWs) with  $\mathbf{q} = \mathbf{q}_3$  are even lower in energy. This deficiency of the DFT can, however, be put to a good use by mapping the DFT (i.e., mean field) energetics onto a spin-Hamiltonian, as it is often done, for instance, for Fe-based superconductors.<sup>40</sup> Since the isotropic and anisotropic magnetic interactions entails completely different energy scales, and require different level of accuracy, we have chosen two different techniques to calculate them; as discussed below, the isotropic calculations were performed perturbatively, allowing us to fully account for the long-range, nesting-driven interaction, while the NN exchange interactions were calculated by brute force comparing highly accurate energy values in different magnetic configurations.

First, we have calculated the Heisenberg part of the Hamiltonian, defined as:

$$H_H = - \sum_{(i \neq j)} J_{ij} \mathbf{M}_i \cdot \mathbf{M}_j, \quad (1)$$

where  $\mathbf{M}_i$  is the Ru moment on the site  $i$ , and the summation is performed over all bonds up to a given coordination sphere. The parameters are calculated in the disordered local moments (DLM) approximation,<sup>41</sup> which is used to model the paramagnetic state of  $\text{Sr}_2\text{RuO}_4$  (see “Methods” for more details and employed approximations).

The results presented in the Fig. 1 are derived for the Ru local moment being fixed to  $1 \mu_B$  in the DLM state. The obtained values of the exchange constants, however, are fairly independent of the values of the local moment fixed in the DLM state; the minimum of the Fourier transform is always at  $\mathbf{q} = (\alpha, \alpha, 0)$  with  $\alpha = 0.3 - 0.31$ . Note that the interplane exchanges nearly vanish, indicating an almost perfect 2D character of the magnetism in  $\text{Sr}_2\text{RuO}_4$ . For instance, the NNs between-the-planes  $J_{001} \approx 0.5 - 1 \text{ K}/\mu_B^2$  (ferromagnetic), or about  $-0.01 J_{200}$ .

The leading term is the in-plane third NN antiferromagnetic interaction  $J_{200}$ , which is quite counterintuitive from the point of view of the Hubbard-model and superexchange mechanism that is often employed as a starting point. This is a consequence of the Ru electrons itinerancy, since  $\text{Sr}_2\text{RuO}_4$  is a metal. The lattice Fourier transform,  $J(\mathbf{q})$ , of the calculated interactions is shown in the Fig. 1b.  $J(\mathbf{q})$  has a meaning of a measure of the energy ( $J(\mathbf{q}) \cdot M^2$ ) of the spin-density fluctuations with a wave-vector  $\mathbf{q}$  and a given amplitude  $M$  [the quantity that is directly related to the static zero-temperature spin susceptibility is  $1/J(\mathbf{q})$ ]. The deep minima of  $J(\mathbf{q})$  at  $\mathbf{q} = (0.31, 0.31, 0) \frac{2\pi}{a}$  suggest that the spin-fluctuations with the wave vector  $\mathbf{q}$  will be dominant in the paramagnetic state of  $\text{Sr}_2\text{RuO}_4$ . The position of these minima is indeed in perfect

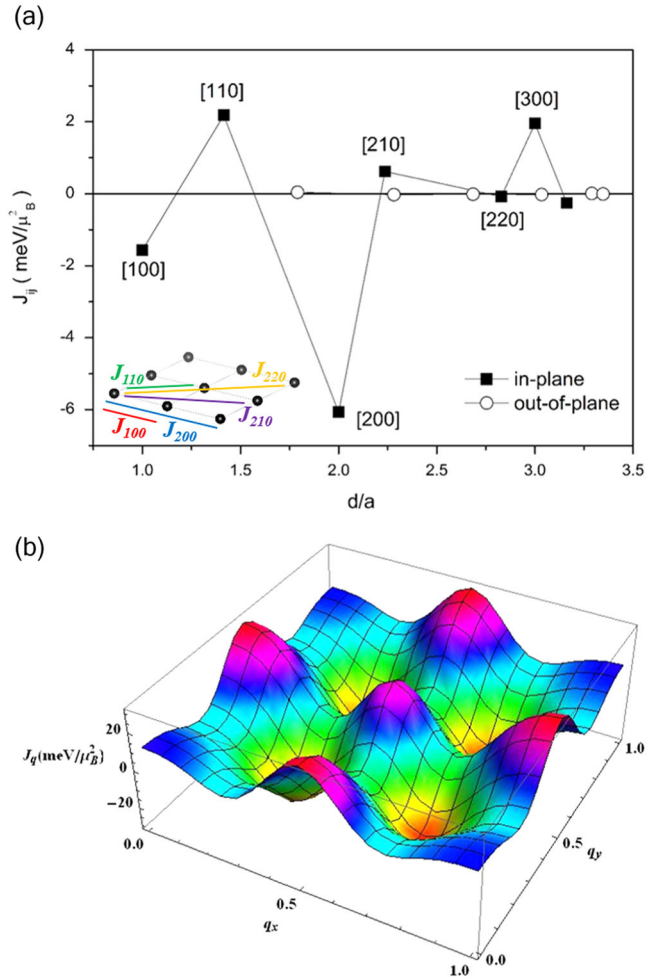


**Fig. 1** Calculated exchange interactions up to the 7th coordination sphere in  $\text{Sr}_2\text{RuO}_4$ . **a** The distance dependence (in terms of planar lattice constant) of isotropic exchange interactions for in-plane (filled square) and out-of-plane (open circle). **b** The Fourier transform of the exchange interactions shown in the panel **a**

agreement with the sharp maxima of the integrated magnetic scattering intensity, experimentally observed in neutron diffraction.<sup>38</sup> Thus, both our calculation and the experiment suggest the dominance of the spin-fluctuations with the wave vector  $\mathbf{q}_3$  in the excitation spectra of  $\text{Sr}_2\text{RuO}_4$ .

In order to extract the relevant anisotropic exchange interaction parameters, we used direct calculations of the total energy in different magnetic configurations compatible with the ordering vector  $\mathbf{q}_3$ . Note that anisotropic magnetic interactions appear exclusively due to the SO coupling (see “Methods” for the description of codes and approximations used in these calculations). Allowed anisotropic terms for the NN terms are absorbed in the following Hamiltonian (simplified compared to a more complete expression discussed in the “Methods” section):

$$H_{IH} = H_H + \sum_{\langle nm \rangle} J^{zz} M_i^z M_j^z + \sum_{\langle nmx \rangle} J^{xy} (M_i^x M_j^x - M_i^y M_j^y) + \sum_{\langle nny \rangle} J^{xy} (M_i^y M_j^y - M_i^x M_j^x), \quad (2)$$

where the first term is given by Eq. (1), the second is Ising exchange (sometimes called the Kitaev interaction), and the last two represent the compass term. Summation in the last two terms

is over all horizontal and all vertical bonds, respectively, while in the Ising term it is over all inequivalent bonds. Note that Dzyaloshinskii-Moriya terms<sup>42, 43</sup> are not allowed by symmetry.

The six most energetically favorable states are depicted in Fig. 2. The first three states can be described as harmonic SDWs:

$$\mathbf{M}_{ijk} = m\mathbf{A} \exp(-i\mathbf{R}_{ijk} \cdot \mathbf{q}_3), \quad (3)$$

where  $\mathbf{A}_a = [-\frac{1}{2}, \frac{\sqrt{3}}{2}, 0]$ ,  $\mathbf{A}_b = [\frac{i}{2\sqrt{2}}, -\frac{i}{2\sqrt{2}}, \frac{1}{2}]$ ,  $\mathbf{A}_c = [\frac{i}{2\sqrt{2}}, \frac{i}{2\sqrt{2}}, \frac{1}{2}]$ , with  $m$  hardly varying between the three states and equal to  $0.76 \mu_B$ . The fourth to sixth states are collinear where the amplitude of the moments varies along each of the crystallographic directions 100, 010, and 110 as  $m'$ ,  $-m'/2$ ,  $-m'/2$  (more precisely, 1.07,  $-0.56$ ,  $-0.56 \mu_B$ ). Note that  $m'$  is very close to  $\sqrt{2}m$  in the harmonic SDWs, and the average  $\langle \mathbf{M}^2 \rangle$  is the same in all these states (within a 1.3% error). In this collinear state the direction of the magnetization can be selected in three inequivalent ways, namely, along 110,  $1\bar{1}0$ , or 001. Upon inclusion of the SO term, the 001 collinear up-up-down structure is the ground state (Table 1).

Next, we fit the energy differences in Table 1 to the Hamiltonian (Eq. (2)), extracting  $J^{zz}$  and  $J^{xy}$  (the fitting procedure included more parameters than in Eq. (2), and is discussed in the “Methods” section). All isotropic (Heisenberg) parts of the exchange interactions are included in the  $H_{IH}$ . The compass parameter  $J^{xy}$  does not affect the states with  $\mathbf{q} \propto (1, 1, 0)$ , and was extracted from a separate set of calculations with  $\mathbf{q}_2 = (0, 1, 0)\frac{\pi}{a}$  and  $\mathbf{M}_{ijk} = m\mathbf{A} \exp(-i\mathbf{R}_{ijk} \cdot \mathbf{q}_2)$ , where  $\mathbf{A}_\perp = (1, 0, 0)$  and  $\mathbf{A}_\parallel = (0, 1, 0)$ ,

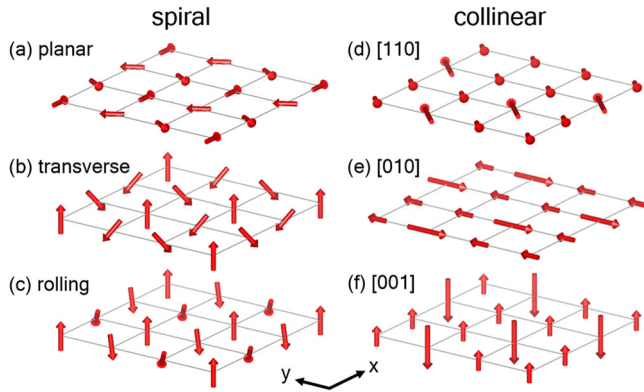


**Fig. 2** Lowest energy magnetic structures ( $\mathbf{q} = (1, 1, 0)\frac{2\pi}{3a}$ ) of  $\text{RuO}_2$  basal plane in  $\text{Sr}_2\text{RuO}_4$ . The **a–c** structures represent different types of spiral magnetic order and **d–f** corresponds to the collinear up-up-down magnetic order with different moment directions

**Table 1.** Calculated total energies (meV/Ru) of various states with the  $\mathbf{q}_3 = (1, 1, 0)\frac{2\pi}{3a}$  periodicity

$q$	Spin orientation	Energy
$(1, 1, 0)(2\pi/3a)$	Planar	0
	Rolling	$-0.42$
	Transverse	$-0.22$
$(1, 1, 0)(2\pi/3a)$	(110)	$-0.34$
	(010)	$-0.24$
	(001)	$-1.27$
$(1, 0, 0)(\pi/a)$	Collinear	38.06
	Stripes	39.57

Note: For spiral phases, the magnitude of the calculated local moments is  $0.76 \mu_B$ , for collinear up-up-down phase is  $0.57 \mu_B$ , and  $1.03 \mu_B$  is for up and down spin, respectively

and  $m$  was fixed to be equal to its value in the spiral states,  $0.76 \mu_B$ . These wave vectors define so-called single stripe antiferromagnetic order, well known in Fe-based superconductors.

Thus, obtained parameters are  $J^{zz} = -1.2 \pm 0.6 \text{ meV}/\mu_B^2$  and  $J^{xy} = 1.0 \text{ meV}/\mu_B^2$  ( $J^{zz}m^2 = -0.70 \pm 0.35 \text{ meV}$ ,  $J^{xy} = 0.57 \text{ meV}$ , for  $m = 0.76 \mu_B$ ). The details of the fitting are described in the “Methods” section. Note that  $J^{xy}$  does not have an error bar not because it was accurately determined, but because we did not have enough calculations to estimate the error. First, one observes that the scale of the anisotropy induced by SO is of the order of 10 K. As discussed in the introduction, this renders the explanation of the invariance of the Knight shift below  $T_c$  in term of the order parameter rotation<sup>10</sup> untenable and shakes the main argument in favor of the chiral triplet superconductivity in  $\text{Sr}_2\text{RuO}_4$ . Second, our fitting provides a powerful tool for modeling normal and especially superconducting properties of  $\text{Sr}_2\text{RuO}_4$  from an entirely different perspective. Compared to the generally accepted models based on the Hubbard-Hund Hamiltonians, our new approach is based entirely on first-principles calculations, and emphasizes the role of magnetic interactions. The corresponding DFT-inspired model Hamiltonian reads:

$$H = H_{IH} + H_e, \quad (4)$$

$$H_e = \sum_{\mathbf{k}as} \epsilon_{\mathbf{k}a} c_{\mathbf{k}as}^\dagger c_{\mathbf{k}as} - I \sum_{\mathbf{k}qas's'} c_{\mathbf{k}-\mathbf{q},as}^\dagger \mathbf{M}_q \cdot \sigma_{ss'} c_{\mathbf{k}as'}, \quad (5)$$

where the first term is the non-interacting energy, with the band (spin) indices  $a$  ( $s$ ), and the second is the Hund’s rule (Stoner, in the DFT parlance) coupling. All electron–electron interactions carried by spin fluctuations are absorbed in the local Hund’s interaction  $I$  and the intersite magnetic interactions  $H_{IH}$ , while interactions due to charge fluctuations are not included in Eq. (5), but can be added separately, if needed (or just collected in one Coulomb pseudopotential  $\mu^*$ , as in the Eliashberg theory). Equation (5) can be understood as a generalized double-exchange Hamiltonian.<sup>44</sup> Indeed, this model, inspired by DFT calculations, entails electrons moving in the same effective potential as used in other techniques, and described by the same tight-binding parameters. However, as it is usual in DFT, all electron–electron interactions are implicitly integrated out. Instead, we introduce quasi-local magnetic moments that interact with the electrons via the local Hund’s rule coupling (parameterized as the Stoner parameter in DFT), while the moments interact among themselves according to the sum of the long-range Heisenberg and the short-range anisotropic Hamiltonian (Eq. (2)). The former part incorporates implicitly all Fermi surface effects, including nesting at  $\mathbf{q} = \{0.3, 0.3, 0\}\frac{2\pi}{a}$ , while the latter selects between different triplet states. It is important not to attempt to integrate out the free carriers  $c_{\mathbf{k}as}$  in Eq. (5) in order to extract additional interaction between the local moments  $\mathbf{M}$ ; that would have been incorrect, because all such interactions had been computed previously and embedded in  $H_{IH}$ . On the contrary, the intended solution of these equations is integrating out the  $\mathbf{M}$ ’s in order to obtain the effective pairing interaction, as illustrated below.

It might be instructive to demonstrate how Eqs. (4) and (5) can be reduced to a Hamiltonian including only the itinerant electrons (as convenient for analyzing superconductivity). We can safely assume that all  $J$ s are much smaller than  $I$ , introduce the itinerant spin polarization  $\mathbf{s}_{ia} = \sum_{s's'} c_{ias}^\dagger \sigma_{ss'} c_{ias'}$ , and single out the terms relevant to the pairwise interaction between  $\mathbf{s}_{ia}$  and  $\mathbf{s}_{j\beta}$ :

$$E_{ij,\alpha\beta} = -I\mathbf{M}_i \cdot \mathbf{s}_{i\alpha} - I\mathbf{M}_j \cdot \mathbf{s}_{j\beta} - J_{ij}\mathbf{M}_i \cdot \mathbf{M}_j. \quad (6)$$

In the lowest order in  $J$ , the mean field solution requires that  $\mathbf{M}_i$  and  $\mathbf{s}_{i\alpha}$  be parallel,  $E_{ij,\alpha\beta} = -2IMS - J_{ij}M^2 \hat{\mathbf{s}}_{i\alpha} \cdot \hat{\mathbf{s}}_{j\beta}$ , and the effective pairwise interaction can be written as  $-J_{ij}M^2 \hat{\mathbf{s}}_{i\alpha} \cdot \hat{\mathbf{s}}_{j\beta}$  (note that essentially the same Hamiltonian, only written in the orbital basis rather than the band basis, which can also be done in this case,

**Table 2.** Relative change in pairing interaction for spin-triplet pairing channels due to Ising and compass exchange terms

Pairing channel		$\delta V/2$
$(\sin k_x \pm i \sin k_y) \hat{z}$	Axial chiral	$J^{zz}$
$\sin k_x \hat{x} + \sin k_y \hat{y}$	Planar radial	$-J^{zz} + 2J^{xy}$
$\sin k_x \hat{y} + \sin k_y \hat{x}$	Planar quadrupolar	$-J^{zz} - 2J^{xy}$
$\sin k_x \hat{x} - \sin k_y \hat{y}$	Planar quadrupolar	$-J^{zz} + 2J^{xy}$
$\sin k_x \hat{y} - \sin k_y \hat{x}$	Planar tangential	$-J^{zz} - 2J^{xy}$

was applied to Fe-based superconductors in several papers, for instance, in ref. 45; after summation of the total energy over the band indices  $\alpha, \beta$  these approaches become equivalent). In principle, one can easily derive the next-order correction to the interaction, which is  $+(J_{ij}^2 M^3 / I_s) (\hat{s}_{i\alpha} \cdot \hat{s}_{j\beta})^2$ .

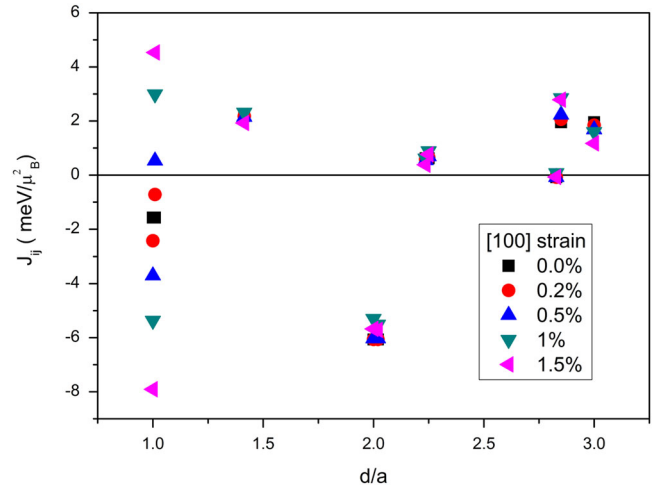
As an example of how this Hamiltonian can be used to address superconductivity, we solve in the simplest mean field approximation the problem of the relative energetics of the five unitary  $p$ -triplet states. In particular, beginning with  $H = -J_{ij} M^2 \hat{s}_{i\alpha} \cdot \hat{s}_{j\beta}$  and restricting the electronic spins to a single band for simplicity (generalizing onto three bands with realistic dispersions is straightforward), we find that the Ising and compass exchange modify the pairing interaction  $\delta V$  in different pairing channels differently, as shown in Table 2.

Thus, in this approximation the five states split into two planar doublets (of course, this degeneracy is not driven by symmetry, and will be lifted in more sophisticated calculations, but likely the splitting will be small) and a  $CpS$  singlet, which is located between the doublets if  $J_{zz} > -|J_{xy}|$  and below both of them otherwise (note that we found  $J_{zz}$  to be negative). In other words, we have shown that selection between chiral and planar superconductivity is driven by the competition between the Ising and compass anisotropic exchange. Of course, this is just an illustration of principle; in principle, this approach should be applied to the true three-band electronic structure and extended to singlet as well as triplet states, but this is beyond the scope of this paper.

We reiterate that we do not insist that this approach is *superior* to the Hubbard-Hamiltonian, but it is *different* and *complementary*, having the potential to uncover new physics. Similar to the former, it can be used in the contexts of, e.g., random-phase approximation, FLEX, or functional renormalization group calculations.

A final note relates to the recent experiments on strained  $Sr_2RuO_4$ . This is a large topic mostly outside of the scope of this paper. However, we would like to make one comment in this regard. The fact that  $T_c$  rapidly grows with the strain and peaks at the strain corresponding to the Lifshits transition (where the  $y$  band touches the X-point) can be explained by either a DOS effect (van Hove singularity) or by a change in pairing interaction. The former explanation, as mentioned before, is realistic for singlet, but not triplet pairing symmetries. The latter would be viable if the changes in DOS were sufficient to shift the balance between the AF and FM tendencies toward the latter. To verify that, we have repeated the calculations of the Heisenberg parameters in the strained case. However, we found that the main effect of the strain is not related to the van Hove singularity, and that the average exchange coupling does not become more ferromagnetic. Instead, the strain introduces a splitting between  $J_{1a}$  and  $J_{1b}$ , while the average value barely changes, as shown in Fig. 3. These results therefore indicate that the peak in  $T_c$  is directly related to the peak in DOS, and not *via* enhanced pairing interaction. This conclusion is supported by recently reported thermodynamic results (see Note), which strongly suggest that not only  $T_c$ , but also  $\Delta C/T_c$  is peaked at the van Hove singularity.

To summarize, we have presented first-principles calculations of the leading isotropic and anisotropic magnetic interactions in


**Fig. 3** Same as Fig. 1a, but as a function of uniaxial strain. Only the nearest neighbor exchange constant is affected by the strain (split into  $J_a$  and  $J_b$ ) at a noticeable level

$Sr_2RuO_4$ . Our results indicate that rotating a  $p$ -wave superconducting order parameter during measurements of the Knight shift is impossible by several orders of magnitude, and thus the invariance of the Knight shift across the transition remains an unresolved puzzle. We further proposed a model framework, based on a double-exchange type Hamiltonian, and incorporating the calculated magnetic interactions in their entirety, and present an example of using this framework for addressing superconducting pairing symmetry.

## METHODS

### First-principles calculations

For relativistic total energy calculations we have employed the projector augmented wave method<sup>46</sup> as implemented in the Vienna Ab initio Simulation Package,<sup>47</sup> including SO coupling.<sup>48</sup> We have used the DFT within the Perdew–Burke–Ernzerhof parametrization for the exchange and correlation potential,<sup>49</sup> and the experimental lattice structure is employed in all calculations. The energy cutoff was set to 400 eV with convergence criteria of  $10^{-6}$  eV. We used up to 1386 irreducible  $k$ -points, reduced to 900 for the four formula units cell. For Ru, a pseudopotential with  $p$ -states included as valence states was selected.

For the calculation of the isotropic exchange constants we used the Korringa–Kohn–Rostokker method within the atomic sphere approximation<sup>50</sup> and the Green function-based magnetic-force theorem.<sup>51</sup> The implementation of this technique has been described elsewhere.<sup>52</sup> Physically, this technique can be considered to be a magnetic analogue of the disordered alloys theory based on coherent potential approximation<sup>52</sup> and is known as the DLM approximation.<sup>41, 53</sup> Upon fixing the Ru magnetic moments in the DLM state we achieved self-consistency using 115 irreducible  $k$ -points in the Brillouin zone, and then used an extended set of  $k$ -points (1529) to compute the isotropic exchange constants in the framework of the magnetic force theorem.

### Fitting procedure

The full equation used to describe the calculated energies, including all bilinear terms up to the second neighbors, reads:

$$H_r = \sum_i K(M_i^z)^2 + \sum_{\langle nn \rangle} J_1^{zz} M_i^z M_j^z + \sum_{\langle 100 \rangle} J_1^{xy} (M_i^x M_j^x - M_i^y M_j^y) + \sum_{\langle 010 \rangle} J_1^{xy} (M_i^y M_j^y - M_i^x M_j^x) \quad (7)$$

$$+ \sum_{\langle nnn \rangle} J_2^{zz} M_i^z M_j^z + \sum_{\langle 110 \rangle} J_2^{xy} (M_i^x M_j^x - M_i^y M_j^y) + \sum_{\langle 1\bar{1}0 \rangle} J_2^{xy} (M_i^y M_j^y - M_i^x M_j^x) \quad (8)$$

**Table 3.** Energies of various calculated magnetic states and the corresponding coefficients in Eq. (7). Magnetic moments are described as  $\mathbf{M}_{ijk} = \text{Re}[m\mathbf{A} \exp(-i\mathbf{R}_{ijk} \cdot \mathbf{q}_z)]$ 

		$\mathbf{A}$	$m$	Energy
Spiral	Planar	$\{1, -i, 0\}$	1	0
	Rolling	$\left\{\frac{i}{\sqrt{2}}, \frac{i}{\sqrt{2}}, 1\right\}$	1	$(K - J_{zz})/2 + J_2^z/4 - 3J_2^{xy}/4$
	Transverse	$\left\{\frac{i}{\sqrt{2}}, -\frac{i}{\sqrt{2}}, 1\right\}$	1	$(K - J_{zz})/2 + J_2^z/4 + 3J_2^{xy}/4$
	(110)	$\left\{\frac{i}{\sqrt{2}}, \frac{i}{\sqrt{2}}, 0\right\}$	$\sqrt{2}, 1/\sqrt{2}$	$-3J_2^{xy}/2$
Collinear	(100)	$\{-1, 0, 0\}$	$\sqrt{2}, 1/\sqrt{2}$	0
	(001)	$\{0, 0, -1\}$	$\sqrt{2}, 1/\sqrt{2}$	$K - J_{zz} + J_2^z/2$

Here, for completeness, we have included the single-site anisotropy term  $K$ ; since it always enters in the same combination with  $J^{zz}$ , they cannot be decoupled within this set of calculations. While this term is, in principle, allowed because of itinerancy, we note that the calculated magnetization is close to the  $S = 1/2$  and therefore we expect  $K \ll J^{zz}$ . This approximation was used in the main text. We have also included, besides the NN anisotropic interaction  $J_1^z$  and  $J_1^{xy}$ , the corresponding second NN interactions  $J_2^z$  and  $J_2^{xy}$ . The latter distinguishes between the collinear state polarized along the (110) tetragonal direction and the one polarized along (100), and the transverse and rolling spirals. We found it to be relatively small,  $0.17 \pm 0.05 \text{ meV}/\mu_B^2$ . The second NN Ising interaction  $J_2^z$  simply adds to  $J^{zz}$ , and therefore was absorbed into the latter in the fitting procedure. The difference in energies between the planar spiral and the (100) collinear structure, 0.24 meV, is likely related to the fact that the isotropic exchange constants enter these two states differently. Our non-relativistic calculations find them degenerate within the computational accuracy, apparently, fortuitously. Since SOC also affects the isotropic constants, it is no surprise that relativistic effects break this accidental degeneracy.

One can calculate  $K - J^{zz}$  and  $J_2^{xy}$  either from the set of spiral calculations, or from collinear calculations; the results differ by  $\pm 30\%$ . It is unlikely that this is due to computational inaccuracy, but rather to other interactions not accounted for, such as third neighbors (which is the leading isotropic exchange) or anisotropic biquadratic coupling.

The full summary of the magnetic patterns and their energies used for the fitting, as well as the expressions for the total energies in terms of the parameters in Eq. (8), are presented in Table 3.

### Mean-field comparison of pairing energies

To find the interactions in Table 2, we begin with the following Hamiltonian  $H_{int}$  that includes charge and spin fluctuations. As an example of how this approach can be used we ask a relatively simple question of how the magnetic anisotropy we have found affects spin-triplet pairing states. To this end, we generalize ref. 54 and consider only a single band with the following Hamiltonian with charge,  $\rho(q)$ , and spin,  $S_i(q)$ , interactions:

$$\begin{aligned}
 H_{int} &= \sum_q \left[ U(q)\rho(q)\rho(-q) + \sum_i J_i(q)S_i(q)S_i(-q) \right] \\
 &= \sum_{k,k'} \sum_q a_{k+q/2,s}^\dagger a_{-k+q/2,s}^\dagger a_{-k'+q/2,m'} a_{k'+q/2,m} \\
 &\times \left[ \rho(k-k')\delta_{s,m}\delta_{s',m'} + J_z(k-k')\sigma_{s,m}^z\sigma_{s',m'}^z \right. \\
 &\quad \left. + J_x(k-k')\sigma_{s,m}^x\sigma_{s',m}^x + J_y(k-k')\sigma_{s,m}^y\sigma_{s',m}^y \right]
 \end{aligned}$$

Focussing on superconductivity with zero momentum Cooper pairs,  $H_{int}$  can be rewritten as:

$$H_{int} = \frac{1}{2} \sum_{k,k'} \left[ V_s(k-k')s_k^\dagger s_{k'}^\dagger + \sum_{i=x,y,z} V_{t,i}(k-k')t_{i,k}^\dagger t_{i,k'}^\dagger \right],$$

where  $s_k = \sum_{s,s'} (i\sigma_y)_{s,s'} c_{-k,s} c_{k,s'}$  and  $t_{i,k} = \sum_{s,s'} (i\sigma_y)_{s,s'} c_{-k,s} c_{k,s'}$  are the

possible singlet and triplet Cooper pair operators, and the effective interactions for the different pairing channels are found to be

$$V_s = \rho(k-k') - J_x(k-k') - J_y(k-k') - J_z(k-k')$$

$$V_{t,x} = \rho(k-k') - J_x(k-k') + J_y(k-k') + J_z(k-k')$$

$$V_{t,y} = \rho(k-k') + J_x(k-k') - J_y(k-k') + J_z(k-k')$$

$$V_{t,z} = \rho(k-k') + J_x(k-k') + J_y(k-k') - J_z(k-k').$$

This result reduces to that found when spin interactions are isotropic<sup>54, 55</sup> or have uniaxial symmetry.<sup>56</sup> In our case, the specific form of the spin anisotropy is

$$J_z = 2J_{z0} \left[ \cos(k_x - k'_x) + \cos(k_y - k'_y) \right]$$

$$J_x = 2J_{\perp 0} \left[ \cos(k_x - k'_x) - \cos(k_y - k'_y) \right]$$

$$J_y = 2J_{\perp 0} \left[ \cos(k_y - k'_y) - \cos(k_x - k'_x) \right].$$

Expressing  $H_{int}$  with the above spin anisotropy in terms of irreducible representations of tetragonal symmetry for the Cooper pairs leads to Table 2.

### Data availability

The authors declare that all source data supporting the findings of this study are available within the paper.

### ACKNOWLEDGEMENTS

B.K., S.K., and C.F. were supported by the joint FWF and Indian Department of Science and Technology (DST) project INDOX (I1490-N19), and by the FWF-SFB ViCoM (Grant No. F41). I.I.M. is supported by ONR through the NRL Basic Research Program. D.F.A. was supported by the National Science Foundation Grant DMREF-1335215.

### AUTHOR CONTRIBUTIONS

S.K. and I.M. conceived the research; B.K. has carried out most of the numerical calculations with contributions by S.K. and I.M.; the superconductivity-related discussion was authored by D.A., who also performed the sample mean-field calculations, and by I.M. All authors participated in the discussions and contributed to writing the paper; C.F. supervised the Vienna part of the project.

## ADDITIONAL INFORMATION

**Competing interests:** The authors declare no competing financial interests.

**Publisher's note:** Springer Nature remains neutral with regard to jurisdictional claims in published maps and institutional affiliations.

## REFERENCES

1. Mackenzie, A. P. & Maeno, Y. The superconductivity of  $\text{Sr}_2\text{RuO}_4$  and the physics of spin-triplet pairing. *Rev. Mod. Phys.* **75**, 657–712 (2003).
2. Ishida, K. et al. Anisotropic pairing in superconducting  $\text{Sr}_2\text{RuO}_4$ : Ru NMR and NQR studies. *Phys. Rev. B* **56**, R505–R508 (1997).
3. Ishida, K. et al. Spin-triplet superconductivity in  $\text{Sr}_2\text{RuO}_4$  identified by  $^{17}\text{O}$  Knight shift. *Nature* **396**, 658–660 (1998).
4. Duffy, J. A. et al. Polarized-neutron scattering study of the cooper-pair moment in  $\text{Sr}_2\text{RuO}_4$ . *Phys. Rev. Lett.* **85**, 5412–5415 (2000).
5. Luke, G. M. et al. Time-reversal symmetry-breaking superconductivity in  $\text{Sr}_2\text{RuO}_4$ . *Nature* **394**, 558–561 (1998).
6. Rice, T. M. & Sigrist, M.  $\text{Sr}_2\text{RuO}_4$ : an electronic analogue of  $^3\text{He}$ ? *J. Phys. Condens. Matter* **7**, L643–L648 (1995).
7. Mazin, I. I. & Singh, D. J. Ferromagnetic spin fluctuation induced superconductivity in  $\text{Sr}_2\text{RuO}_4$ . *Phys. Rev. Lett.* **79**, 733–736 (1997).
8. Mazin, I. I. & Singh, D. J. Competitions in layered ruthenates: ferromagnetism versus antiferromagnetism and triplet versus singlet pairing. *Phys. Rev. Lett.* **82**, 4324–4327 (1999).
9. Braden, M. et al. Inelastic neutron scattering study of magnetic excitations in  $\text{Sr}_2\text{RuO}_4$ . *Phys. Rev. B* **66**, 064522 (2002).
10. Murakawa, H., Ishida, K., Kitagawa, K., Mao, Z. Q. & Maeno, Y. Measurement of the  $^{101}\text{Ru}$ -Knight shift of superconducting  $\text{Sr}_2\text{RuO}_4$  in a parallel magnetic field. *Phys. Rev. Lett.* **93**, 167004 (2004).
11. Xia, J., Maeno, Y., Beyersdorf, P. T., Fejer, M. M. & Kapitulnik, A. High resolution polar Kerr effect measurements of  $\text{Sr}_2\text{RuO}_4$ : evidence for broken time-reversal symmetry in the superconducting state. *Phys. Rev. Lett.* **97**, 167002 (2006).
12. Nelson, K. D., Mao, Z. Q., Maeno, Y. & Liu, Y. Odd-parity superconductivity in  $\text{Sr}_2\text{RuO}_4$ . *Science* **306**, 1151–1154 (2004).
13. Žutić, I. & Mazin, I. Phase-sensitive tests of the pairing state symmetry in  $\text{Sr}_2\text{RuO}_4$ . *Phys. Rev. Lett.* **95**, 217004 (2005).
14. Matano, K., Kriener, M., Segawa, K., Ando, Y. & Zheng, G.-Q. Spin-rotation symmetry breaking in the superconducting state of  $\text{Cu}_x\text{Bi}_2\text{Se}_3$ . *Nat. Phys.* **12**, 852–854 (2016).
15. Yonezawa, S. et al. Thermodynamic evidence for nematic superconductivity in  $\text{Cu}_x\text{Bi}_2\text{Se}_3$ . *Nat. Phys.* **13**, 123–126 (2017).
16. Yip, S.-K. Models of superconducting  $\text{Cu}_x\text{Bi}_2\text{Se}_3$ : single- versus two-band description. *Phys. Rev. B* **87**, 104505 (2013).
17. Fu, L. Odd-parity topological superconductor with nematic order: application to  $\text{Cu}_x\text{Bi}_2\text{Se}_3$ . *Phys. Rev. B* **90**, 100509 (2014). (R).
18. Matsumoto, M. & Sigrist, M. Quasiparticle states near the surface and the domain wall in a  $p_x \pm ip_y$ -wave superconductor. *J. Phys. Soc. Jpn.* **68**, 994–1007 (1999).
19. Kallin, C. & Berlinsky, A. J. Is  $\text{Sr}_2\text{RuO}_4$  a chiral p-wave superconductor? *J. Phys. Condens. Matter* **21**, 164210 (2009).
20. Scaffidi, T. & Simon, S. H. Large Chern number and edge currents in  $\text{Sr}_2\text{RuO}_4$ . *Phys. Rev. Lett.* **115**, 087003 (2015).
21. Kirtley, J. R. et al. Upper limit on spontaneous supercurrents in  $\text{Sr}_2\text{RuO}_4$ . *Phys. Rev. B* **76**, 014526 (2007).
22. Agterberg, D. F. Vortex lattice structures of  $\text{Sr}_2\text{RuO}_4$ . *Phys. Rev. Lett.* **80**, 5184–5187 (1998).
23. Mineev, V. P. Superconducting phase transition of  $\text{Sr}_2\text{RuO}_4$  in a magnetic field. *Phys. Rev. B* **89**, 134519 (2014).
24. Gor'kov, L. P. Anisotropy of the upper critical field in exotic superconductors. *JETP Lett.* **40**, 1155–1158 (1984).
25. Amano, Y., Ishihara, M., Ichioka, M., Nakai, N. & Machida, K. Pauli paramagnetic effects on mixed-state properties in a strongly anisotropic superconductor: application to  $\text{Sr}_2\text{RuO}_4$ . *Phys. Rev. B* **91**, 144513 (2015).
26. Hicks, C. W. et al. Strong increase of  $T_c$  of  $\text{Sr}_2\text{RuO}_4$  under both tensile and compressive strain. *Science* **344**, 283–285 (2014).
27. Hassinger, E. et al. Vertical line nodes in the superconducting gap structure of  $\text{Sr}_2\text{RuO}_4$ . *Phys. Rev. X* **7**, 011032 (2017).
28. Maeno, Y., Kittaka, S., Nomura, T., Yonezawa, S. & Ishida, K. Evaluation of spin-triplet superconductivity in  $\text{Sr}_2\text{RuO}_4$ . *J. Phys. Soc. Jpn.* **81**, 011009 (2012).
29. Ng, K. K. & Sigrist, M. The role of spin-orbit coupling for the superconducting state in  $\text{Sr}_2\text{RuO}_4$ . *Europhys. Lett.* **49**, 473–479 (2000).

30. Eremin, I., Manske, D. & Bennemann, K. H. Electronic theory for the normal-state spin dynamics in  $\text{Sr}_2\text{RuO}_4$ : anisotropy due to spin-orbit coupling. *Phys. Rev. B* **65**, 220502 (2002). (R).
31. Annett, J. F., Györfy, B. L., Litak, G. & Wysokiński, K. I. Magnetic field induced rotation of the  $d$ -vector in the spin-triplet superconductor  $\text{Sr}_2\text{RuO}_4$ . *Phys. Rev. B* **78**, 054511 (2008).
32. Cobo, S., Ahn, F., Eremin, I. & Akbari, A. Anisotropic spin fluctuations in  $\text{Sr}_2\text{RuO}_4$ : role of spin-orbit coupling and induced strain. *Phys. Rev. B* **94**, 224507 (2016).
33. Scaffidi, T., Romers, J. S. & Simon, S. H. Pairing symmetry and dominant band in  $\text{Sr}_2\text{RuO}_4$ . *Phys. Rev. B* **89**, 220510 (2014).
34. Veenstra, C. N. et al. Spin-orbital entanglement and the breakdown of singlets and triplets in  $\text{Sr}_2\text{RuO}_4$  revealed by spin- and angle-resolved photoemission spectroscopy. *Phys. Rev. Lett.* **112**, 127002 (2014).
35. Sidis, Y. et al. Evidence for incommensurate spin fluctuations in  $\text{Sr}_2\text{RuO}_4$ . *Phys. Rev. Lett.* **83**, 3320–3323 (1999).
36. Servant, F. et al. Magnetic excitations in the normal and superconducting states of  $\text{Sr}_2\text{RuO}_4$ . *Phys. Rev. B* **65**, 184511 (2002).
37. Braden, M. et al. Anisotropy of the incommensurate fluctuations in  $\text{Sr}_2\text{RuO}_4$ : a study with polarized neutrons. *Phys. Rev. Lett.* **92**, 097402 (2004).
38. Iida, K. et al. Inelastic neutron scattering study of the magnetic fluctuations in  $\text{Sr}_2\text{RuO}_4$ . *Phys. Rev. B* **84**, 060402 (2011). (R).
39. de Boer, P. K. & de Groot, R. A. Electronic structure of magnetic  $\text{Sr}_2\text{RuO}_4$ . *Phys. Rev. B* **59**, 9894–9897 (1999).
40. Glasbrenner, J. K. et al. Effect of magnetic frustration on nematicity and superconductivity in iron chalcogenides. *Nat. Phys.* **11**, 953–958 (2015).
41. Györfy, B. L., Pindor, A. J., Staunton, J., Stocks, G. M. & Winter, H. A first-principles theory of ferromagnetic phase transitions in metals. *J. Phys. F Met. Phys.* **15**, 1337–1386 (1985).
42. Dzyaloshinskii, I. E. A thermodynamic theory of weak ferromagnetism of anti-ferromagnetics. *J. Phys. Chem. Solids* **4**, 241–255 (1958).
43. Moriya, T. Anisotropic superexchange interaction and weak ferromagnetism. *Phys. Rev.* **120**, 91–98 (1960).
44. Khomskii, D. I. *Basic Aspects of the Quantum Theory of Solids* (Cambridge University Press, 2010).
45. Seo, K., Bernevig, B. A. & Hu, J. P. Pairing symmetry in a two-orbital exchange coupling model of oxypnictides. *Phys. Rev. Lett.* **101**, 206404 (2008).
46. Blöchl, P. E. Projector augmented-wave method. *Phys. Rev. B* **50**, 17953–17979 (1994).
47. Kresse, G. & Furthmüller, J. Efficient iterative schemes for *ab initio* total-energy calculations using a plane-wave basis set. *Phys. Rev. B* **54**, 11169–11186 (1996).
48. Steiner, S., Khmelevskiy, S., Marsmann, M. & Kresse, G. Calculation of the magnetic anisotropy with projected-augmented-wave methodology and the case study of disordered  $\text{Fe}_{1-x}\text{Co}_x$  alloys. *Phys. Rev. B* **93**, 224425 (2016).
49. Perdew, J. P., Burke, K. & Ernzerhof, M. Generalized gradient approximation made simple. *Phys. Rev. Lett.* **77**, 3865–3868 (1996).
50. Ruban, A. V. & Skriver, H. L. Calculated surface segregation in transition metal alloys. *Comp. Mater. Sci.* **15**, 143–199 (1999).
51. Liechtenstein, A. I., Katsnelson, M. I., Antropov, V. P. & Gubanov, V. A. Local spin density functional approach to the theory of exchange interactions in ferromagnetic metals and alloys. *J. Magn. Magn. Mater.* **67**, 65–74 (1987).
52. Ruban, A. V., Shallockross, S., Simak, S. I. & Skriver, H. L. Atomic and magnetic configurational energetics by the generalized perturbation method. *Phys. Rev. B* **70**, 125115 (2004).
53. Cyrot, M. Phase transition in Hubbard model. *Phys. Rev. Lett.* **25**, 871–874 (1970).
54. Miyake, K., Schmitt-Rink, S., & Varma, C. M. Spin-fluctuation-mediated even-parity pairing in heavy-fermion superconductors. *Phys. Rev. B* **34**, 6554 (1986).
55. Cho, W., Thomale, R., Raghu, S. & Kivelson, S. A. Band structure effects on the superconductivity in Hubbard models. *Phys. Rev. B* **88**, 064505 (2013).
56. Kuwabara, T., & Ogata, M. Spin-Triplet Superconductivity due to Anti-ferromagnetic Spin-Fluctuation in  $\text{Sr}_2\text{RuO}_4$ . *Phys. Rev. Lett.* **85**, 4586–4589 (2000).



**Open Access** This article is licensed under a Creative Commons Attribution 4.0 International License, which permits use, sharing, adaptation, distribution and reproduction in any medium or format, as long as you give appropriate credit to the original author(s) and the source, provide a link to the Creative Commons license, and indicate if changes were made. The images or other third party material in this article are included in the article's Creative Commons license, unless indicated otherwise in a credit line to the material. If material is not included in the article's Creative Commons license and your intended use is not permitted by statutory regulation or exceeds the permitted use, you will need to obtain permission directly from the copyright holder. To view a copy of this license, visit <http://creativecommons.org/licenses/by/4.0/>.

© The Author(s) 2017